Aerosol and Air Quality Research, 17: 1975–1984, 2017

ISSN: 1680-8584 print / 2071-1409 online
doi: 10.4209/aaqr.2017.05.0189

Particulate Size Distribution and Sources Evaluation of *n*-Alkanes during Long-Term Haze Episode around Chaohu Lake, Eastern China

Qiu-Ping Xu[1], Ji-Zhong Wang[1*], Jia-Qin Liu[2], Shu-Chuan Peng[1]

[1] *School of Resources and Environmental Engineering, Hefei University of Technology, Hefei 230009, China*
[2] *Institute of Industry and Equipment Technology, Hefei University of Technology, Hefei 230009, China*

ABSTRACT

n-Alkanes (from nC_{16} to nC_{32}) associated with particulate matters were determined in the ambient air around Chaohu Lake, Eastern China, from October to December in 2014 during a long-term haze episode. The total concentrations of particle bounded *n*-alkanes varied from 332 to 2500 ng m^{-3}, with the homologues of nC_{24}–nC_{30} the most abundant species. Spatial analysis revealed that low concentrations of *n*-alkanes existed at the sites close to Chaohu Lake, while high concentrations were generally at locations distant from the lake. For all aggregated fractions, most *n*-alkanes were distributed in fine particles with the mean geometric mean diameter (GMD) varying from 3.0 ± 0.6 μm for nC_{16} to 2.1 ± 0.6 μm for nC_{32}. Short chain *n*-alkanes were accumulated in coarse particles with a unimodal distribution, but long chain aliphatic hydrocarbons appeared to have a biomodal distribution in fine and coarse particles. The mass size distribution of individual *n*-alkane homologue was predominantly influenced by its volatility; thus GMDs were well correlated with the logarithmically transformed subcooled liquid vapor pressures (P_L^o, Pa) of *n*-alkanes at each sampling site, following the equation: $GMDs = m_g Log P_L^o + b_g$. Furthermore, m_g and b_g obtained from all locations tended to exhibit a significant linear correlation. This suggests that all saturated aliphatic hydrocarbons follow a similar accumulation mode during a haze episode, which allows us to predict the size distribution and GMD of a compound based on its P_L^o.

Keywords: Chaohu Lake; *n*-alkanes; particulate matter; size distribution; geometric mean diameter.

INTRODUCTION

With rapid economic growth and industrial development over the past three decades, China has experienced increasing environmental deterioration. Air pollution has become one of the most significant environmental and human health problems because overwhelming haze has frequently covered China's major cities in recent years and tens of millions people have suffered from high inhalation exposure to various air pollutants (Jiang *et al.*, 2015; Li *et al.*, 2015b). Atmospheric aerosol particles, especially those with an aerodynamic diameter less than 2.5 μm ($PM_{2.5}$), have been confirmed as vital air pollutants. These aerosols can not only be emitted from various anthropogenic sources including fossil fuel combustion, biomass burning, motor vehicles, but also formed from atmospheric reactions of organic volatile compounds or inorganic precursor gases (Yue *et al.*, 2016' Cao *et al.*, 2017). Natural mechanical processes including volcanic eruptions, wind-driven or traffic-related suspension of road, soil, and mineral dust, sea salt are also the important contributors to aerosol particles (Li *et al.*, 2015a; Farahat *et al.*, 2016). The atmospheric aerosols are generally composed of sulfate, nitrate, ammonium, sea salt, mineral dust, organic matter, and black or elemental carbon (Bzdek *et al.*, 2012; Calvo *et al.*, 2013). Organic matters such as aliphatic hydrocarbons are the important fraction of aerosol particles, usually accounting for 20–50% of total mass (Simoneit *et al.*, 1991).

Aerosol particles can vary greatly in size (from less than 1 nm to 100 μm). The particles with different sizes are generally considered from different origins. Ultrafine particles (< 0.1 μm) can be emitted directly from various combustors or formed in the atmosphere by homogeneous nucleation. Fine particles ($PM_{2.5}$) can arise from combustion or formation from atmospheric reactions, whereas coarse particles are generally from the resuspension of dust or soil. Particle size is the key determining factor in the environmental behavior of aerosols and thus influences residence time, removal mechanisms, adsorption capacity and reaction activation. Both ultrafine and coarse particles are susceptible to be removed from atmosphere and have relatively short life-time. Ultrafine particles are easy to coagulate to form large sizes of particles and coarse particles can be removed by dry deposition during the transport,

* Corresponding author.
Tel.: 86-551-2901523; Fax: 86-551-63621485
E-mail address: wangjizh@hfut.edu.cn

whereas fine particle can reside in atmosphere for a long period of time. As a result, the particles size distributions of aerosols from emission sources to background areas change gradually (Offenberg and Baker, 1999). Furthermore, due to large specific surface areas, fine particles have higher binding affinity to metals and semi-volatile organic compounds when compared with coarse particles (Offenberg and Baker, 2000; Karanasiou *et al.*, 2007). Interaction and partitioning between the gas and particle phase also depend on particle size (Kadowaki, 1994; Fraser *et al.*, 1997). For example, less volatile organic compounds such as polycyclic aromatic hydrocarbons are more likely associated with fine particles (Hien *et al.*, 2007; Ladji *et al.*, 2014). More importantly, particle size greatly influences the health impacts of aerosols because fine particles can penetrate deep into lungs and bloodstream. Thus the size of particles which is usually described by their aerodynamic diameter (geometric mean diameter, GMD) has a key influence on their properties, chemical composition, fate and environmental/health impacts. Research on the size of aerosol particles and their chemical compositions is critical to the understanding of their atmospheric properties and effects on health and to the elucidation of their sources and environmental sinks. Most available studies were conducted to investigate the particle size distribution of PAHs (Offenberg and Baker, 1999; Hien *et al.*, 2007), *n*-alkanes (Karanasiou *et al.*, 2007), inorganic elements (Balachandran *et al.*, 2000) and water-soluble compounds (Bao *et al.*, 2009) in urban and rural areas, but knowledge has remained limited in the size distribution of particle bounded *n*-alkanes in typical haze episodes.

Therefore, the main purpose of this work was to elucidate the distribution of saturated aliphatic hydrocarbons (*n*-alkanes) associated with size segregated atmospheric aerosols collected around Chaohu Lake, Eastern China, during a long-term haze pollution episode. Additionally, we aimed to investigate whether the volatility of individual target compound affects its mass size distribution.

MATERIALS AND METHODS

Study Areas and Samples Collection

In the present study, eleven sampling locations around Chaohu Lake were selected to collect the airborne particles during a long-term haze episode from October to December in 2014. These sampling sites included Changfeng city (CF), Xiaomiao town (XM), Emerald Lake campus of Hefei University of Technology (GDXQ), Feidong city (FD), Hefei NO.1 High School (YZ), Sanhe town (SH), Zhongmiao town (ZM), Chaohu city (CH), Sanbing town (SB), Tangchi village (TC) and Lujiang city (LJ) (Table S1 and Fig. 1). Generally, CF, FD, CH, and LJ are located in the downtown areas of the cities; GDXQ and YZ in the suburban areas of Hefei City; XM, SH, ZM, and SB in the central areas of cities; and TC in a rural area. It should be noted that SH is a typical tourist area. Generally, these sampling sites were distributed evenly around Chaohu Lake, allowing us to characterize the distribution of *n*-alkanes around Chaohu Lake.

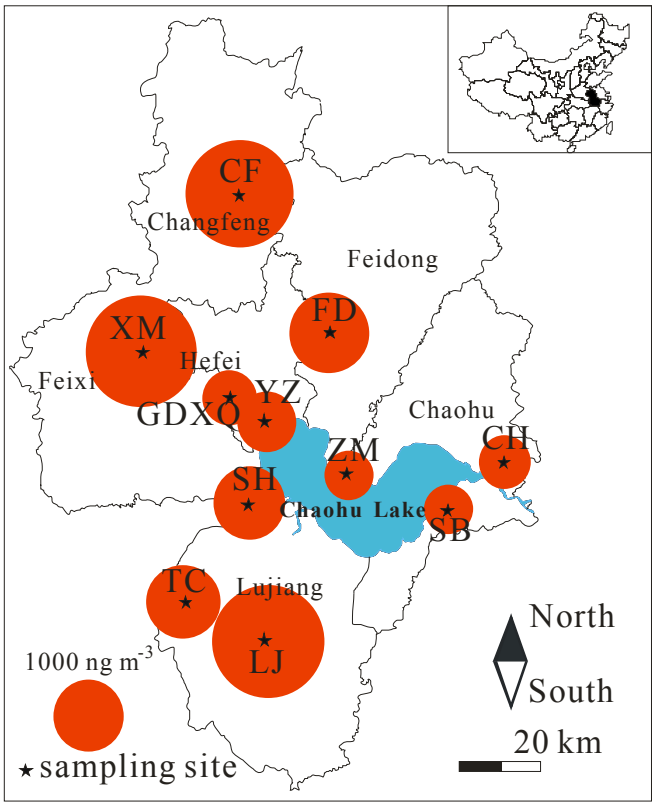

Fig. 1. The spatial variation on the atmospheric particle bounded *n*-alkanes around Chaohu Lake. The area of circle represents the summed concentrations (ng m^{-3}) of all *n*-alkanes homologues.

Air samples were collected using an eight-stage no*n*-viable impactor (Anderson, Franklin, Massachusetts, USA) for a period of 72 hours. The impactor was deployed on the top of the buildings with a height of 5–30 m (Table S1). Except for GDXQ and YZ where the samplers were on the top of university buildings, the remaining samplers were placed on the top of hotel buildings. Airborne particles were sampled at a flow rate of 28.3 L min^{-1} and the cutoff aerodynamic diameters for each stage were 0.4–0.7, 0.7–1.1, 1.1–2.1, 2.1–3.3, 3.3–4.7, 4.7–5.8, 5.8–9.0, and > 9.0 μm.

Before sampling, glass fiber filters (Whatman International, Maidstope, UK) were baked in a muffle at 400°C for 4 hours to remove residual organic matters and then weighed. The filters after sampling were weighed again and packed with aluminum foils and stored at –20°C until analysis. For *n*-alkanes analysis, fiber filters were cut into small pieces, spiked with nC_{24}–d_{50} as recovery surrogates, and then Soxhlet extracted with 100 mL of a mixture of *n*-hexane and dichloromethane (1:1, v/v) for 48 hours. The extract was concentrated to about 1 mL and cleaned through a glass column packed with cotton, 3 g of silica gel and 1 g of anhydrous sodium sulfate from bottom to top. The final eluant was concentrated to about 1 mL and spiked with a known amount of internal standard (nC_{30}–d_{62}) prior to instrumental analysis.

The quantitation and quantification of the target compounds were performed with a Model 7890A gas chromatograph (GC) coupled with a Model 5975C mass spectrometer (MS) (Agilent Technologies, USA). Gas chromatographic separation was performed on a 30-m DB-5MS capillary column (30 m × 0.25 mm, internal diameter; 0.25 μm film thickness). The MS was operated with an electronic impact (EI) mode at 70 eV using selected-io*n*-monitoring (SIM). The MS ion source and quadrupole temperature were set as 300°C and 180°C respectively. The injection volume was 1 μL and the injection was performed in splitless mode at 300°C. The oven temperature was programmed from 60 to 180°C at a rate of 8 °C min^{-1}, to 220 °C at a rate of 2 °C min^{-1}, and then to 320°C at a rate of 8 °C min^{-1}.

Quality Assurance

All samples were spiked with surrogate standard to monitor the recovery of sample extraction. A method blank was included with every batch of 20 samples. The recoveries of surrogate standards ranged from 54.3 to 136%. Reported concentrations were not corrected with recovery efficiency.

Data Analysis

Carbon preference index (CPI), an important indicator of *n*-alkanes sources, is defined as the ratio of the total *n*-alkanes with odd carbon number to those with even carbon numbers. It is usually used to differentiate the contribution of biogenic organics from anthropogenic emission.

$$CPI = \frac{\sum odd\left(nC_{16} - nC_{32}\right)}{\sum even\left(nC_{16} - nC_{32}\right)} \quad (1)$$

In general, *n*-alkanes are considered to be from biological origins if a CPI value is greater than 3.0, whereas they are inferred from anthropogenic sources if a CPI value is close to unit (Simoneit, 1989).

Apart from this, the contribution of plant wax deriving *n*-alkanes can be calculated with the following equation to determine the relative importance of biogenic or petrogenic sources (Wang *et al.*, 2012):

$$\%\mathrm{Wax}C_n = \frac{\sum\left[C_n - \frac{1}{2}\left(C_{n-1} + C_{n+1}\right)\right]}{\sum\left(C_{15} - C_{34}\right)} \quad (2)$$

where $\%\mathrm{Wax}C_n$ (ng m^{-3}) is the concentration of plant wax *n*-alkanes and negative values are taken as zero. C_n, C_{n-1} and C_{n+1} are the concentrations of *n*-alkanes with neighboring carbon numbers. When the compositional characteristics of *n*-alkanes exhibit a shape of jaggedness, *n*-alkanes usually have a greater $\%\mathrm{Wax}C_n$ which suggests biological sources as the main source. If an odd to even preference doesn't exist and $\%\mathrm{Wax}C_n$ is smaller, it usually indicates the main source of anthropogenic emission.

Geometric mean diameter (GMD) was applied to describe the size distribution of *n*-alkanes in this study and determined using the below equation:

$$\mathrm{LogGMD} = \frac{\sum\left(C_i \times \log D_{p,i}\right)}{\sum C_i} \quad (3)$$

where C_i is the concentration of *n*-alkanes in size class *i* and $D_{p,i}$ is the geometric mean particle diameter collected on stage *i* (Offenberg and Baker, 1999).

RESULTS AND DISCUSSION

Mass Concentration of n-Alkanes around Chaohu Lake

According to the data released by the air quality monitoring stations of Hefei (http://www.pm25x.com/city/hefei.htm), the air quality index (AQI), $PM_{2.5}$ and PM_{10} contents varied in ranges of 54.9–238, 37.3–187 ng m^{-3} and 49.5–296 ng m^{-3}, respectively (Table S1). The recorded highest daily aerosol concentrations were 187 μg m^{-3} for $PM_{2.5}$ and 296 μg m^{-3} for PM_{10}, respectively, approximately twice the daily average standard of 65 μg m^{-3} for $PM_{2.5}$ and 150 μg m^{-3} for PM_{10} regulated by the United States Environmental Protection Agency (U.S. EPA).

All *n*-alkane homologues from nC_{16} to nC_{32} were detectable in all samples collected around Chaohu Lake. Aggregate particle-associated *n*-alkanes (sum of all size fractions or ΣAK) varied from 476 to 2500 ng m^{-3} with an arithmetic mean of 1220 ± 812 ng m^{-3}. SB was observed with the lowest summed concentration, and samples collected in ZM, GDXQ, YZ and CH also contained relatively low levels, generally less than 1000 ng m^{-3}. However, the concentrations in SH, CF, XM, LJ, TC and FD were relatively higher with the maximum value in LJ, where the sampling site was located at a downtown area. Therefore, a general spatial distribution pattern was observed, i.e., low *n*-alkanes concentrations at

the sites close to Chaohu Lake and high concentrations in the locations distant from the lake (Fig. 1). Relatively low *n*-alkanes concentrations in the sampling sites close to Chaohu Lake were partly associated with the different features of wind speed which was also important to the haze formation. Previous studies indicated that high particular matter concentrations were frequently observed in the meteorological condition with low wind speeds (Jiang *et al.*, 2015; Li *et al.*, 2015b). The average $PM_{2.5}$ concentrations recorded in Binhu Monitor Station (close to the YZ site) during the entire sampling period was significantly lower than that in Luyang Monitor Station (close to the CF site, $p < 0.05$) and the mean value in Gaoxin Monitor Station (close to the XM site, $p < 0.05$) (Fig. 2). Spatial variation in the summed *n*-alkanes concentrations could also be attributed to the open straw burning and residual coal combustion in the outlying regions of the city during the sampling period (Wang *et al.*, 2009a; Wang *et al.*, 2009b).

Compositional Characteristics of n-Alkanes around Chaohu Lake

The compositional distributions of *n*-alkanes for all aggregated fractions at eleven sites showed that homologues from nC_{24} to nC_{30} were overall dominant but their abundances were also site dependent (Fig. 3). The carbon number of the most abundant *n*-alkanes (C_{max}) was at nC_{26} in LJ, XM, CF and FD, at nC_{27} in SH and at nC_{29} in the remaining locations. Interestingly, all sites with C_{max} at nC_{26} exhibited a characteristic unimodal *n*-alkane profile, possibly suggesting significant contributions from heavy duty diesel trucks (Pietrogrande *et al.*, 2011). Indeed, these sampling sites were close to the major transits. By contrast, the sites with C_{max} at nC_{27} or nC_{29} had a bimodal distribution of *n*-alkane with the first peak at nC_{17} and the second peak at nC_{27} or nC_{29}, which probably indicated a mixture of sources combining fossil fuel and biomass combustion with weak biogenic and petrogenic signatures (Lin and Lee, 2004). For all sites, the CPI ranged from 1.3 ± 0.2 (site TC) to 1.8 ± 0.5 (site ZM), suggesting significant anthropogenic activities related sources along with minor contribution from vascular plants. The contributions of biogenic wax *n*-alkanes to the total *n*-alkanes concentrations based upon the estimation of $\%WaxC_n$ ranged from 10.5 ± 3.5% (site GDXQ) to 19.5 ± 7.9% (site ZM). Generally, the sample with a relatively higher CPI value usually had a relatively higher $\%WaxC_n$ value, resulting in a significantly positive correlation between these two indicators (Fig. 4).

Compared with other studies, it was clear that the contribution of biogenic sources to particle bounded *n*-alkanes around Chaohu Lake in winter was similar to those reported in other Chinese cities. For instance, the CPI values reported Tianjin (China) in winter ranged from 1.07 to 1.49 and the $\%WaxC_n$ 7.68%–22.69%, which reflected main sources from anthropogenic emission and less significant contributions from higher plants (Wu *et al.*, 2007). Even lower $\%WaxC_n$ values (7 ± 4%–9 ± 5%) were reported in Shanghai (China), revealing even lower contributions from biogenic sources in such a major metropolitan area (Feng *et al.*, 2006).

Size Distribution of n-Alkanes

In the present study, the particles collected on the impactor stages with a diameter less than 2.1 μm were referred to as fine particles, while the particle diameter greater than 2.1 μm represented coarse particles. On average, fine

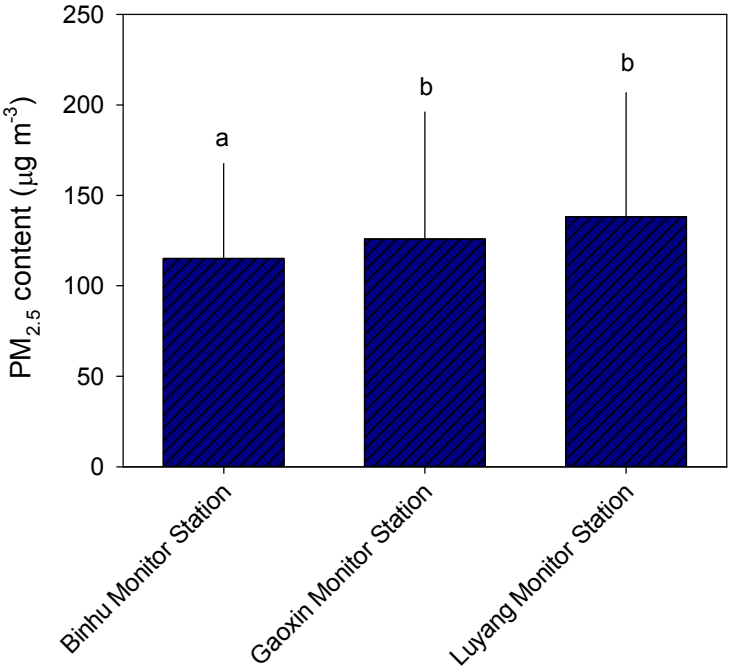

Fig. 2. Daily concentration of $PM_{2.5}$ between Oct to Dec of 2014 from three air quality monitoring stations. Daily concentrations were computed by hourly ambient observation data (http://www.pm25x.com/city/hefei.htm). Different letters within a column indicate significant difference ($p < 0.05$).

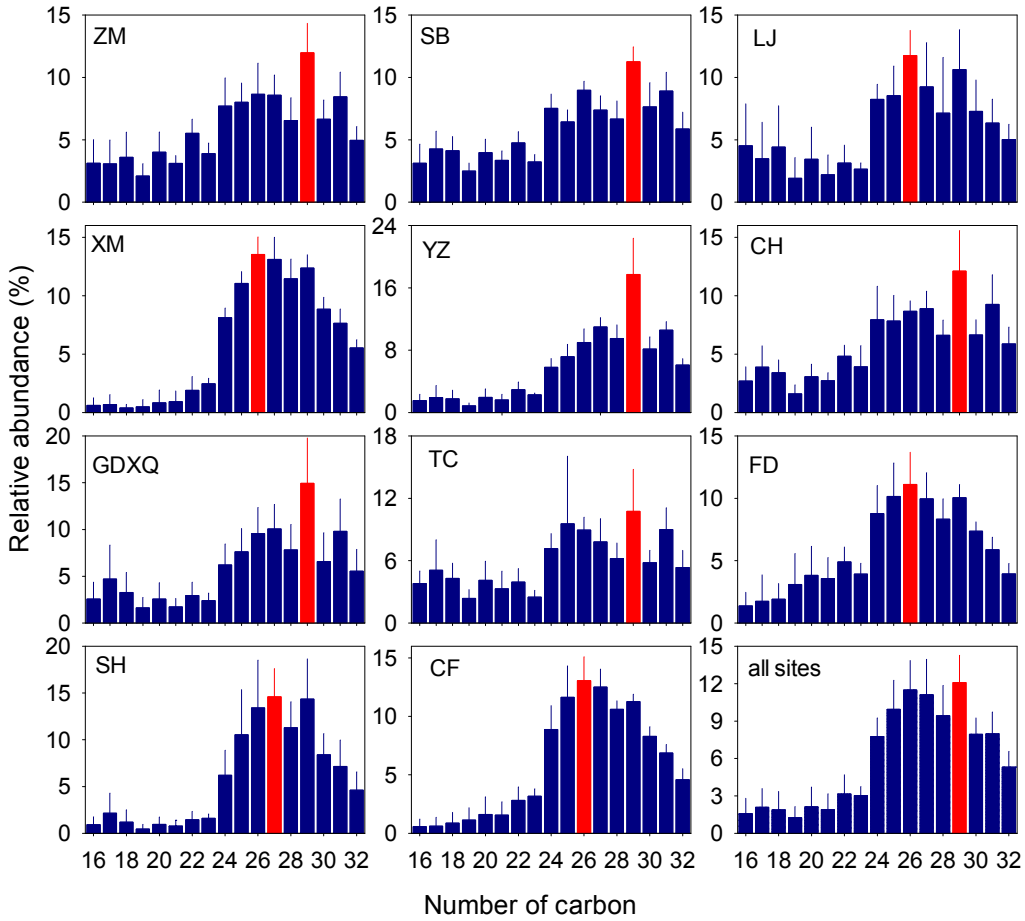

Fig. 3. The relative abundances and standard deviations of *n*-alkane homologues with different number of carbon at 11 sampling sites around Chaohu Lake. Red bar represents the carbon number of the most abundant *n*-alkane homologue (C_{max}).

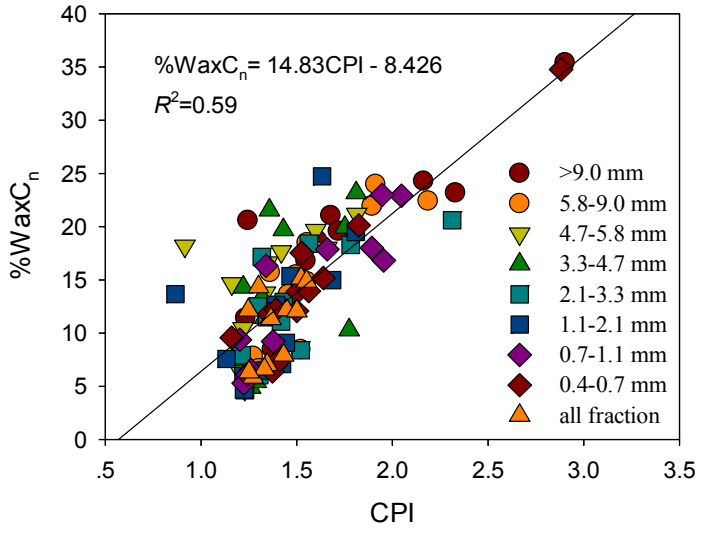

Fig. 4. The correlation between %WaxC$_n$ and CPI.

particles associated *n*-alkanes accounted for 52.1 ± 12.5% of the total concentrations, with the minimal proportion of 46.2% at XM and the maximum proportion of 67.7% at YZ. These results indicated that most *n*-alkanes were distributed in fine particles consistently across sampling sites (Fig. 5). Generally, the fraction with a size of 0.4–0.7 μm contributed the largest percentage of particulate ΣAK contents at ZM and FD. For the samples collected at SB, XM and YZ, most *n*-alkanes were found to be associated to the fraction of 0.7–1.1 μm, accounting for 20.4%, 20.5% and 50.7% of

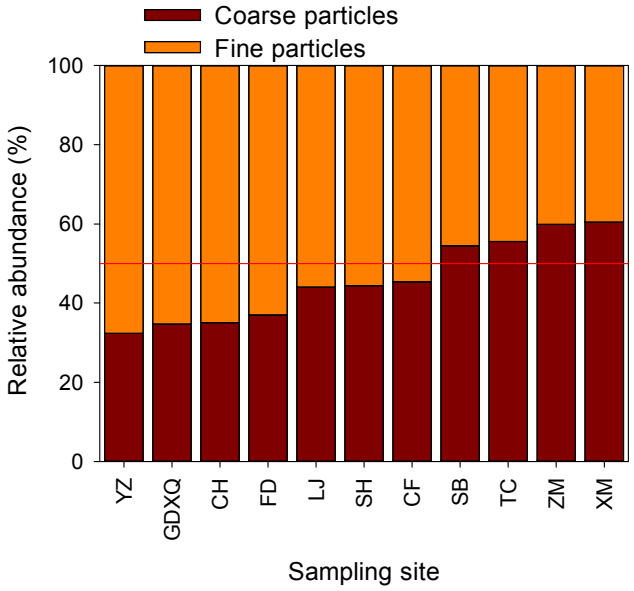

Fig. 5. Relative abundances of summed concentrations of *n*-alkanes in fine and coarse particles from the Chaohu Lake basin.

the total ΣAK contents, respectively. However, *n*-alkanes at TC, LJ, CF, SH, CH and GDXQ were greatly dominated by the fraction of 1.1–2.1 μm with the contribution to the total ΣAK contents of 29.9%, 50.1%, 21.6%, 35.3%, 48.1% and 53.3%, respectively (Fig. 6). Because of the large surface areas of fine particles, contaminants preferentially absorb onto the surface of fine particles by gas-solid distribution equilibrium (Chen *et al.*, 2006; Tian *et al.*, 2011). Previous research also indicated that particles with small sizes were generally enriched with *n*-alkanes and the concentrations of *n*-alkanes in the smallest particles were more than 10 times greater than that in the largest particles (Yassaa *et al.*, 2001; Bi *et al.*, 2005).

Fig. 7 shows the Lundgren diagrams ($dC/Cd\log D_p$ vs D_p) for all samples collected at 11 sites, which is a useful method for comparing the concentrations of coarse and fine particles (Zhu *et al.*, 2014). The *n*-alkanes in all sampling sites with the exception of ZM and SH revealed a bimodal distribution. The fine mode was in the size of 0.7–1.1 μm, occasionally in the range of 0.4–0.7 μm (at SH, YZ and FD). The coarse mode predominantly corresponded to 5.9–9.0 μm. By contrast, *n*-alkanes at the samples from ZM and SH exhibited a unimodal distribution with the peaks at 3.3–5.8 μm and 1.1–3.3 μm, respectively. It should be noted that *n*-alkanes at YZ, GDXQ , SH and CF were mostly accumulated in fine particles, possibly suggesting fossil fuel combustion derived hydrocarbons (Karanasiou *et al.*, 2007). For the samples from the remaining sites, natural sources can also play a role on the size distributions (Ladji *et al.*, 2014).

Additionally, *n*-alkane species with different carbon chain length differed greatly in their associations with fine or coarse particles. Generally, short chain alkanes were accumulated in coarse particles with a unimodal distribution from nC_{16} to nC_{23}, whereas long chain hydrocarbons could be associated with both fine and coarse particles with a

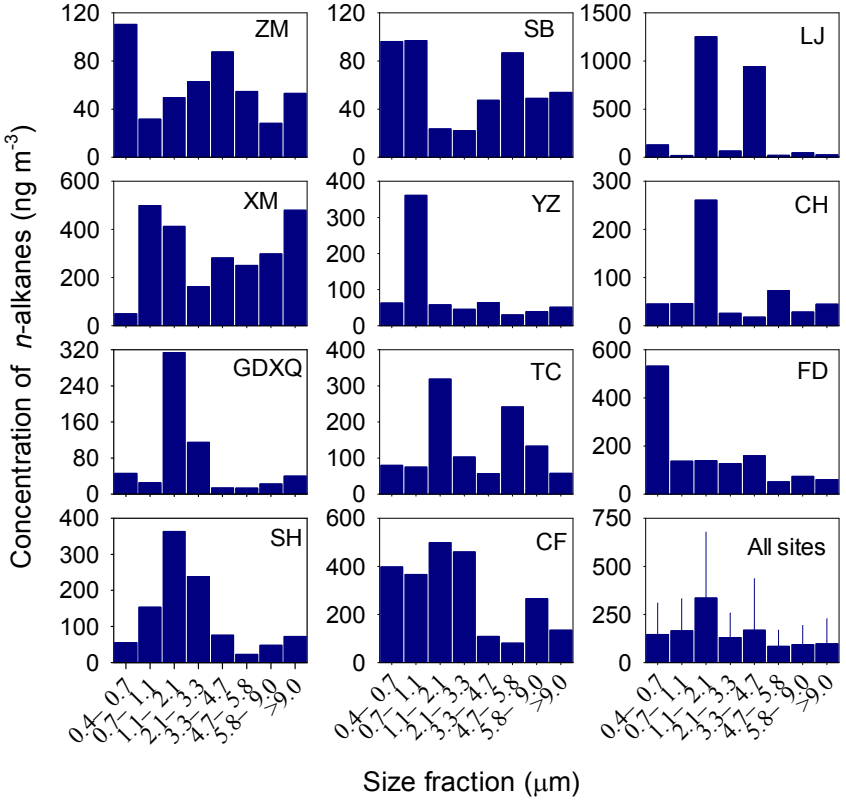

Fig. 6. Concentrations of *n*-alkanes in each size fraction for all sampling sites around the Chaohu Lake basin.

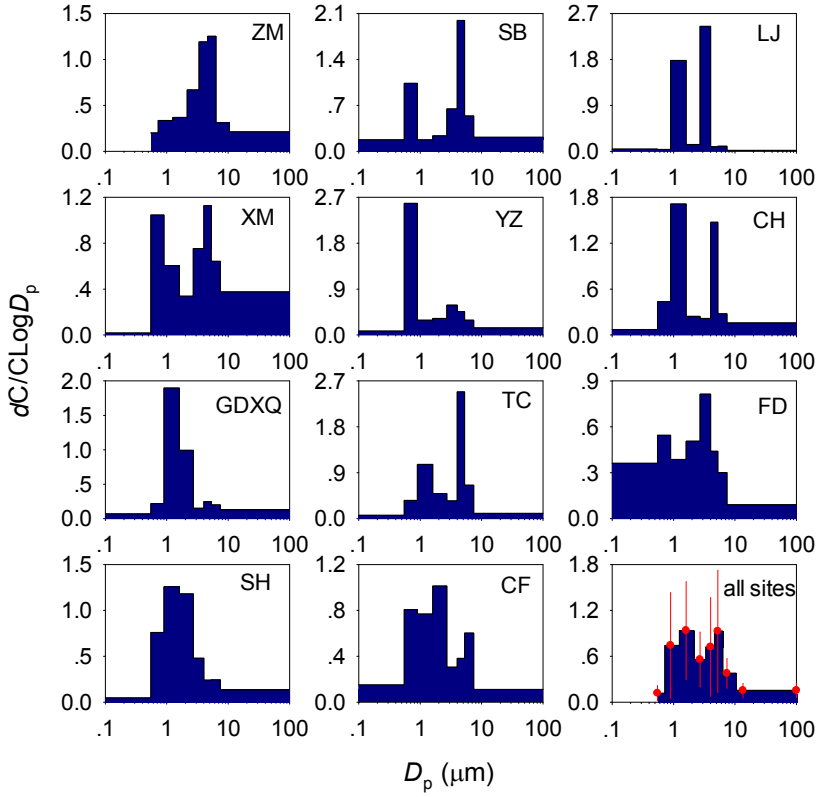

Fig. 7. Size distribution of *n*-alkanes for all sites around Chaohu Lake.

biomodal distribution (Fig. 8). Semi-volatile organic compounds in urban aerosols usually exhibited a biomodal distribution because of primary and second sources, but those in aerosols from long-term transport exhibited a unimodal distribution due to dry deposition of coarse fractions or repartition between gaseous and particulate phases (Offenberg and Baker, 1999). Therefore, significant desorption and re-adsorption occurred for short chain *n*-alkanes. Long chain *n*-alkanes could be from both anthropogenic and natural sources (Bi *et al.*, 2005). Previous studies indicated that hydrocarbons associated with biogenic sources were usually accumulated in coarse fractions (Alves *et al.*, 2000; Bi *et al.*, 2005). Thus high CPI and %WaxC_n values in the coarse fractions (> 9.0 μm) (Fig. 9) at all sampling sites suggested significant contributions from natural sources. The lowest CPI and %WaxC_n values were found in the fraction of 1.1–2.1 μm, likely implying the primary emission from fuel fossil combustion. Interestingly, the finest fraction (0.4–0.7 μm) was determined to include a signature of biogenic wax *n*-alkanes. Indeed, size distribution of semi-volatile organic compounds is controlled by their emitting sources, volatilization/re-adsorption affinities, and meteorological conditions (Cheruiyot *et al.*, 2015). Primary aerosols from fuel fossil and biomass combustion are generally among the smaller fine particles in the atmospheric environment (Offenberg and Baker, 1999).

Geometric Mean Diameters

GMDs varied from 1.1 μm for nC_{25} at FD to 5.3 μm for nC_{20} at XM. Generally, the samples collected at ZM, SB, TC, FD, and XM had larger GMDs than those from the remaining sites. Average GMDs for all samples ranged from 3.0 ± 0.6 μm for nC_{16} to 2.1 ± 0.6 μm for nC_{32}, tending to decrease along with the increasing of the number of carbon. GMDs in all sampling sites with exception of CH positively correlated against logarithmically transformed subcooled liquid vapor pressure ($\mathrm{Log}P_L^o$), whereas the GMD at CH was negatively correlated with $\mathrm{Log}P_L^o$. Thus GMDs could be predicted by $\mathrm{Log}P_L^o$ with a general equation of GMDs = $m_g\mathrm{Log}P_L^o + b_g$. The correlative regressions were significant ($p < 0.05$) at all sites and the values of m_g and b_g were summarized in Table 1. The value of m_g varied from –0.053 to 0.254, which was significantly lower than those obtained for *n*-alkanes in urban aerosols (Offenberg and Baker, 1999). Aerosols in rural areas usually had m_g much less than those in urban areas (Offenberg and Baker, 1999). Our results possibly suggested the aerosols from long-term transport during the haze episode. A significant correlation was found between m_g and b_g (Fig. 10), suggesting a general tendency of the correlation between GMD and $\mathrm{Log}P_L^o$ from a variety of samples collected around Chaohu Lake and the suitability of predicting GMD from P_L^o for a given organic compound.

CONCLUSIONS

Atmospheric particulate matters were collected in 11 locations around Chaohu Lake, Eastern China, from October to December in 2014 using an eight-stage no*n*-viable impactor to determine 17 *n*-alkane homologues (from nC_{16} to nC_{32}).

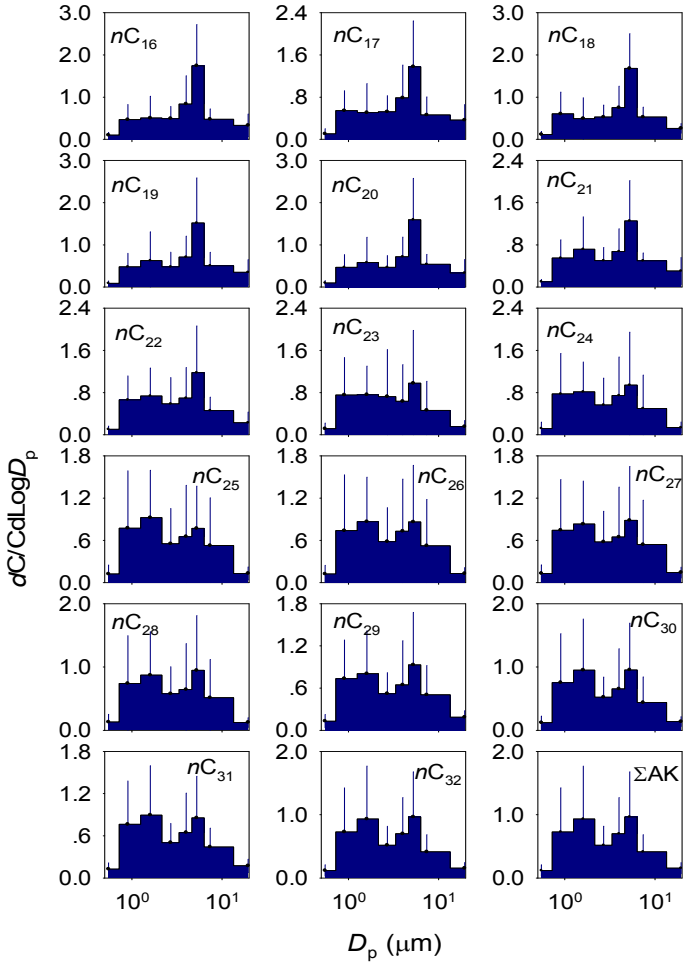

Fig. 8. The distribution of individual *n*-alkanes homologue in fine and coarse particles from the Chaohu Lake basin.

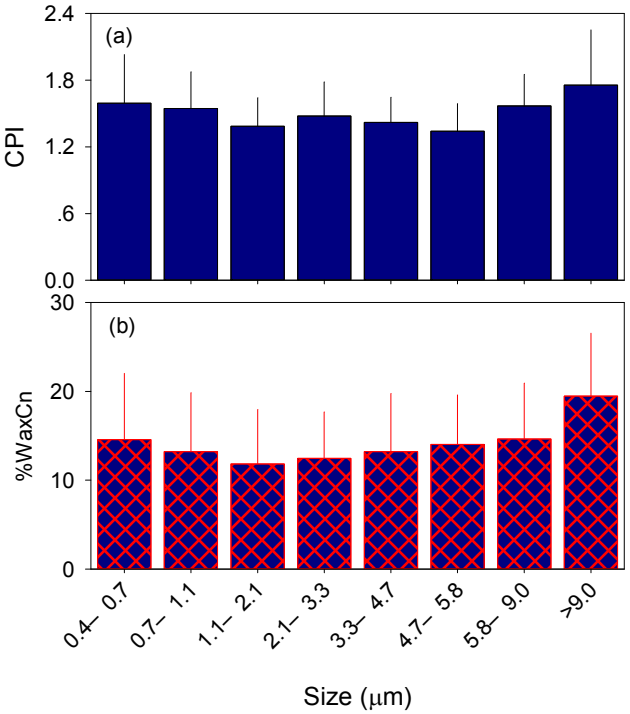

Fig. 9. Size distributions of CPI and %WaxC$_n$ for particle associated *n*-alkanes.

Table 1. Slope (m_g) and intercept (b_g) for the linear regression between geometric mean diameter and log-based subcooled liquid vapor pressure ($Log P_L^o$) (GMD = $m_g Log P_L^o + b_g$). R^2 and p represent the square of regression coefficient and probability value, respectively.

site	$m_g \pm$ error (μm Pa^{-1})	$b_g \pm$ error (μm)	R^2	p
ZM	0.239 ± 0.039	3.714 ± 0.205	0.741	< 0.01
SB	0.099 ± 0.016	2.818 ± 0.085	0.742	< 0.01
TC	0.115 ± 0.025	3.3 ± 0.128	0.628	< 0.01
LJ	0.057 ± 0.1	2.579 ± 0.053	0.712	< 0.01
FD	0.254 ± 0.059	3.153 ± 0.307	0.592	< 0.01
CF	0.171 ± 0.044	3.113 ± 0.23	0.54	< 0.01
XM	0.193 ± 0.077	4.43 ± 0.405	0.323	0.03
SH	0.147 ± 0.031	3.031 ± 0.16	0.642	< 0.01
YZ	0.109 ± 0.04	2.34 ± 0.211	0.358	0.02
CH	–0.053 ± 0.021	1.87 ± 0.112	0.317	0.03
GDXQ	0.129 ± 0.015	2.812 ± 0.078	0.853	< 0.01

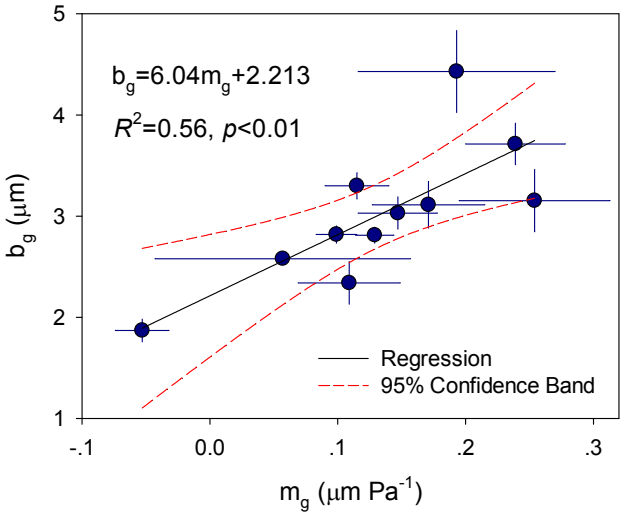

Fig. 10. The correlation between m_g and b_g in the aerosols collected from the Chaohu Lake basin.

Aggregated concentrations of particle-associated *n*-alkanes ranged from 332 to 2500 ng m^{-3}. The sampling sites with lower concentrations were close to Chaohu Lake and higher concentrations occurred at sites distant from the lake. These aliphatic hydrocarbons were predominately from anthropogenic activities along with minor contributions from biogenic source. The *n*-alkanes homologues, nC_{24} to nC_{30}, were dominant in the investigated samples from the study region. Particulate *n*-alkanes were mostly enriched in fine particles with the mean GMD ranging from 3.0 ± 0.6 μm for nC_{16} to 2.1 ± 0.6 μm for nC_{32}. Furthermore, our data demonstrated that $Log P_L^o$ appeared to be an important factor influencing the size distributions of *n*-alkanes. .

ACKNOWLEDGEMENTS

The present study was financially supported by the Fundamental Research Funds for the National Natural Science Foundation of China (41390240) and the Central Universities (2015HGCH0002 and 201510359051).

SUPPLEMENTARY MATERIAL

Supplementary data associated with this article can be found in the online version at http://www.aaqr.org.

REFERENCES

Alves, C.A., Pio, C.A. and Duarte, A.C. (2000). Particulate size distributed organic compounds in a forest atmosphere. *Environ. Sci. Technol.* 34: 4287–4293.

Balachandran, S., Meena, B.R. and Khillare, P.S. (2000). Particle size distribution and its elemental composition in the ambient air of Delhi. *Environ. Int.* 26: 49–54.

Bao, L.F., Sekiguchi, K., Wang, Q.Y. and Sakamoto, K. (2009). Comparison of water-soluble organic components in size-segregated particles between a roadside and a suburban site in Saitama, Japan. *Aerosol Air Qual. Res.* 9: 412–420.

Bi, X.H., Sheng, G.Y., Peng, P.A., Chen, Y.J. and Fu, J.M. (2005). Size distribution of *n*-alkanes and polycyclic aromatic hydrocarbons (PAHs) in urban and rural atmospheres of Guangzhou, China. *Atmos. Environ.* 39: 477–487.

Bzdek, B.R., Pennington, M.R. and Johnston, M.V. (2012). Single particle chemical analysis of ambient ultrafine aerosol: A review. *J. Aerosol Sci.* 52: 109–120.

Calvo, A.I., Alves, C., Castro, A., Pont, V., Vicente, A.M. and Fraile, R. (2013). Research on aerosol sources and chemical composition: Past, current and emerging issues. *Atmos. Res.* 120: 1–28.

Cao, Z.Y., Zhou, X.H., Ma, Y.J., Wang, L.P., Wu, R.D., Chen, B. and Wang, W.X. (2017). The concentrations, formations, relationships and modeling of sulfate, nitrate and ammonium (SNA) aerosols over China. *Aerosol Air Qual. Res.* 17: 84–97.

Chen, L.G., Mai, B.X., Bi, X.H., Chen, S.J., Wang, X.M., Ran, Y., Luo, X.J., Sheng, G.Y., Fu, J.M. and Zeng, E.Y. (2006). Concentration levels, compositional profiles, and gas-particle partitioning of polybrominated diphenyl ethers in the atmosphere of an urban city in south China. *Environ. Sci. Technol.* 40: 1190–1196.

Cheruiyot, N.K., Lee, W.J., Mwangi, J.K., Wang, L.C., Lin,

N.H., Lin, Y.C., Cao, J.J., Zhang, R.J. and Chang-Chien, G.P. (2015). An overview: Polycyclic aromatic hydrocarbon emissions from the stationary and mobile sources and in the ambient air. *Aerosol Air Qual. Res.* 15: 2730–2762.

Farahat, A., El-Askary, H. and Dogan, A.U. (2016). Aerosols size distribution characteristics and role of precipitation during dust storm formation over Saudi Arabia. *Aerosol Air Qual. Res.* 16: 2523–2534.

Feng, J.L., Hu, M., Chan, C.K., Lau, P.S., Fang, M., He, L.Y. and Tang, X.Y. (2006). A comparative study of the organic matter in $PM_{2.5}$ from three Chinese megacities in three different climatic zones. *Atmos. Environ.* 40: 3983–3994.

Fraser, M.P., Cass, G.R., Simoneit, B.R.T. and Rasmussen, R.A. (1997). Air quality model evaluation data for organics. 4. C_2-C_{36} no*n*-aromatic hydrocarbons. *Environ. Sci. Technol.* 31: 2356–2367.

Hien, T.T., Thanh, L.T., Kameda, T., Takenaka, N. and Bandow, H. (2007). Distribution characteristics of polycyclic aromatic hydrocarbons with particle size in urban aerosols at the roadside in Ho Chi Minh City, Vietnam. *Atmos. Environ.* 41: 1575–1586.

Jiang, J.K., Zhou, W., Cheng, Z., Wang, S.X., He, K.B. and Hao, J.M. (2015). Particulate matter distributions in China during a winter period with frequent pollution episodes (January 2013). *Aerosol Air Qual. Res.* 15: 494–503.

Kadowaki, S. (1994). Characterization of carbonaceous aerosols in the Nagoya urban area. 2. Behavior and origin of particulate *n*-alkanes. *Environ. Sci. Technol.* 28: 129–135.

Karanasiou, A.A., Sitaras, I.E., Siskos, P.A. and Eleftheriadis, K. (2007). Size distribution and sources of trace metals and *n*-alkanes in the Athens urban aerosol during summer. *Atmos. Environ.* 41: 2368–2381.

Ladji, R., Yassaa, N., Balducci, C. and Cecinato, A. (2014). Particle size distribution of *n*-alkanes and polycyclic aromatic hydrocarbons (PAHs) in urban and industrial aerosol of Algiers, Algeria. *Environ. Sci. Pollut. Res. Int.* 21: 1819–1832.

Li, R., Gong, J.H., Zhou, J.P., Sun, W.Y. and Ibrahim, A.N. (2015a). Multi-satellite observation of an intense dust event over southwestern China. *Aerosol Air Qual. Res.* 15: 263–270.

Li, Y., Zhao, H.J. and Wu, Y.F. (2015b). Characteristics of particulate matter during haze and fog (pollution) episodes over northeast China, autumn 2013. *Aerosol Air Qual. Res.* 15: 853–864.

Lin, J.J. and Lee, L.C. (2004). Characterization of *n*-alkanes in urban submicron aerosol particles (PM_1). *Atmos. Environ.* 38: 2983–2991.

Offenberg, J.H. and Baker, J.E. (1999). Aerosol size distributions of polycyclic aromatic hydrocarbons in urban and over-water atmospheres. *Environ. Sci. Technol.* 33: 3324–3331.

Offenberg, J.H. and Baker, J.E. (2000). Aerosol size distributions of elemental and organic carbon in urban and over-water atmospheres. *Atmos. Environ.* 34: 1509–1517.

Pietrogrande, M.C., Abbaszade, G., Schnelle-Kreis, J., Bacco, D., Mercuriali, M. and Zimmermann, R. (2011). Seasonal variation and source estimation of organic compounds in urban aerosol of Augsburg, Germany. *Environ. Pollut.* 159: 1861–1868.

Simoneit, B.R.T. (1989). Organic matter of the troposphere-V: Application of molecular marker analysis to biogenic emissions into the troposphere for source reconciliations. *J. Atmos. Chem.* 8: 251–275.

Simoneit, B.R.T., Sheng, G.Y., Chen, X.J., Fu, J.M., Zhang, J. and Xu, Y.P. (1991). Molecular marker study of extractable organic matter in aerosols from urban areas of China. *Atmos. Environ.* 25A: 2111–2129.

Tian, M., Chen, S.J., Wang, J., Shi, T., Luo, X.J. and Mai, B.X. (2011). Atmospheric deposition of halogenated flame retardants at urban, e-waste, and rural locations in southern China. *Environ. Sci. Technol.* 45: 4696–4701.

Wang, G.H., Kawamura, K., Xie, M.J., Hu, S.Y., Cao, J.J., An, Z.S., Waston, J.G. and Chow, J.C. (2009a). Organic molecular compositions and size distributions of Chinese summer and autumn aerosols from Nanjing: characteristic haze event caused by wheat straw burning. *Environ. Sci. Technol.* 43: 6493–6499.

Wang, J.Z., Yang, Z.Y. and Chen, T.H. (2012). Source apportionment of sediment-associated aliphatic hydrocarbon in a eutrophicated shallow lake, China. *Environ. Sci. Pollut. Res.* 19: 4006–4015.

Wang, Z.Z., Bi, X.H., Sheng, G.Y. and Fu, J.M. (2009b). Characterization of organic compounds and molecular tracers from biomass burning smoke in south China I: broad-leaf trees and shrubs. *Atmos. Environ.* 43: 3096–3102.

Wu, S.P., Tao, S., Zhang, Z.H., Lan, T. and Zuo, Q. (2007). Characterization of TSP-bound *n*-alkanes and polycyclic aromatic hydrocarbons at rural and urban sites of Tianjin, China. *Environ. Pollut.* 147: 203–210.

Yassaa, N., Youcef Meklati, B., Cecinato, A. and Marino, F. (2001). Particulate *n*-alkanes, *n*-alkanoic acids and polycyclic aromatic hydrocarbons in the atmosphere of Algiers City Area. *Atmos. Environ.* 35: 1843–1851.

Yue, D.L., Zhong, L.J., Zhang, T., Shen, J., Yuan, L., Ye, S.Q., Zhou, Y. and Zeng, L.M. (2016). Particle growth and variation of cloud condensation nucleus activity on polluted days with new particle formation: A case study for regional air pollution in the PRD region, China. *Aerosol Air Qual. Res.* 16: 323–335.

Zhu, H.W., Wang, Y., Wang, X.W., Luan, T.G. and Tam, N.F.Y. (2014). Distribution and accumulation of polybrominated diphenyl ethers (PBDEs) in Hong Kong mangrove sediments. *Sci. Total Environ.* 468: 130–139.

Received for review, July 11, 2017
Revised, July 25, 2017
Accepted, July 25, 2017